

# Direct detection of dimer orbitals in $\text{Ba}_5\text{AlIr}_2\text{O}_{11}$

Y. Wang,<sup>1,\*</sup> Ruitang Wang,<sup>2,3</sup> Jungho Kim,<sup>4</sup> M. H. Upton,<sup>4</sup> D. Casa,<sup>4</sup>  
T. Gog,<sup>4</sup> G. Cao,<sup>5</sup> G. Kotliar,<sup>1,6</sup> M. P. M. Dean,<sup>1,†</sup> and X. Liu<sup>2,‡</sup>

<sup>1</sup>*Department of Condensed Matter Physics and Materials Science,  
Brookhaven National Laboratory, Upton, New York 11973, USA*

<sup>2</sup>*School of Physical Science and Technology, ShanghaiTech University, Shanghai 201210, China*

<sup>3</sup>*Beijing National Laboratory for Condensed Matter Physics and Institute of Physics,  
Chinese Academy of Sciences, Beijing 100190, China*

<sup>4</sup>*Advanced Photon Source, Argonne National Laboratory, Argonne, Illinois 60439, USA*

<sup>5</sup>*Department of Physics, University of Colorado Boulder, Boulder, Colorado 80309, USA*

<sup>6</sup>*Physics and Astronomy Department, Rutgers University, Piscataway, NJ 08854, USA*

(Dated: October 15, 2018)

The electronic states of many Mott insulators, including iridates, are often conceptualized in terms of localized atomic states such as the famous “ $J_{\text{eff}} = 1/2$  state”. Although, orbital hybridization can strongly modify such states and dramatically change the electronic properties of materials, probing this process is highly challenging. In this work, we directly detect and quantify the formation of dimer orbitals in an iridate material  $\text{Ba}_5\text{AlIr}_2\text{O}_{11}$  using resonant inelastic x-ray scattering (RIXS). Sharp peaks corresponding to the excitations of dimer orbitals are observed and analyzed by a combination of density functional theory (DFT) calculations and theoretical simulations based on a Ir-Ir cluster model. Such partially delocalized dimer states lead to a re-definition of the angular momentum of the electrons and changes in the magnetic and electronic behaviors of the material. We use this to explain the reduction of the observed magnetic moment with respect to prediction based on atomic states. This study opens new directions to study dimerization in a large family of materials including solids, heterostructures, molecules and transient states.

Many of the most interesting phases in correlated quantum materials occur in systems with strong Coulomb repulsion  $U$ , which tends to drive electron localization via the Mott insulating mechanism [1]. Due to this, we often conceptualize the electronic and magnetic properties of these systems in terms of localized states [2], even though many of the most interesting cases occur when there is strong competition between  $U$  and electron hopping  $t$ . Of particular interest in this regard is the localized “ $J_{\text{eff}} = 1/2$  state” in the iridates, which is the conceptual building block for a host of fascinating proposed and observed states including frustrated magnets [3–7], topological insulators [8, 9], and possibly even unconventional superconductors [10]. Hopping between  $\text{IrO}_6$  octahedra delocalizes the electrons and is expected to be relevant in many classes of iridate (or other heavy  $d$ -electron materials) with edge-sharing or face-sharing octahedra [11–16]. This can heavily modify, or even destroy, the  $J_{\text{eff}} = 1/2$  state motivating arguments about how best to conceptualize the electronic state of iridates [11, 17, 18]. Directly probing these states is therefore highly desirable. In the simplest case of dimerization between neighboring pairs of  $\text{IrO}_6$  octahedra one expects the formation of quasi-localized dimer orbitals, which are difficult to probe by photo-emission due to the absence of dispersive bands and hard to probe optically as dipole optical selection rules means that transitions within a orbital manifold are nominally forbidden. RIXS, on the other hand, has been shown as an particularly incisive probe of on-site localized transitions in the iridates, but as far as we are aware, has never definitively isolated an excitation asso-

ciated with dimerization [19, 20].

In this Letter, we establish that RIXS can directly measure peaks associated with orbital dimerization and that a quantitative description of the dimer electronic configuration can be extracted using DFT calculations and multiplet modeling. For this study we employ face-sharing iridate  $\text{Ba}_5\text{AlIr}_2\text{O}_{11}$  and account for how these interactions modify  $J_{\text{eff}} = 1/2$  state expected on the nominally  $5d^5$  atom in this crystal, reproducing the previously measured reduction in the magnetic moment [21]. We argue that, given the proven ability of RIXS to measure molecules, oxide heterostructures and even ultra-fast transient states, this has great potential to probe orbital dimerization under many different circumstances [22–27].

Single crystal samples of  $\text{Ba}_5\text{AlIr}_2\text{O}_{11}$  were synthesized using the self-flux method as described in Refs. [21, 28]. Previous diffraction and transport measurements confirm high sample quality [21].  $\text{Ba}_5\text{AlIr}_2\text{O}_{11}$  forms an orthorhombic unit cell with space group  $Pnma$  (No. 62) with  $a = 18.76$ ,  $b = 5.755$ , and  $c = 11.06$  Å [21]. As shown in Fig. 1(a), two face-sharing  $\text{IrO}_6$  octahedra form isolated dimers, which are then connected by  $\text{AlO}_4$  tetrahedra. These two inequivalently coordinated face-sharing Ir octahedra in a dimer are labeled as Ir1 and Ir2, as shown in Fig. 1(a,b). RIXS experiments were performed at the Ir- $L_3$  edge by using the MERIX instrument at Sector 27 of the Advanced Photon Source [29]. A 2 m Si (884) diced analyzer was used to energy-resolve the scattered x-rays. Different incident beam monochromatization setups were tested before settling with a combined  $\sim 80$  meV total resolution (Full-Width-Half-Maximum).

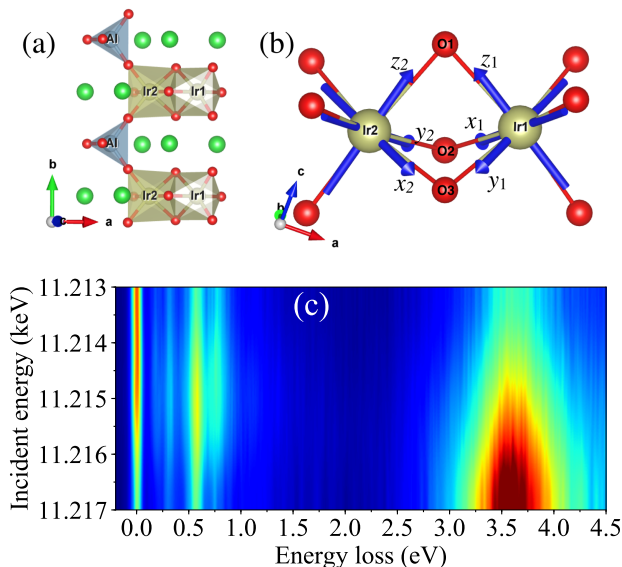


FIG. 1. (a) Crystal structure of Ba<sub>5</sub>AlIr<sub>2</sub>O<sub>11</sub>. The two inequivalent IrO<sub>6</sub> octahedra are labeled Ir1 and Ir2 and colored in dark yellow. Quasi one dimensional Ir chain structures occur via the connection of these octahedra through AlO<sub>4</sub> tetrahedra along the *b*-axis. (b) Illustration of the local Cartesian coordinates used in the definition of *t*<sub>2g</sub> orbitals. The orientation of the local coordinates is chosen such that the *x*, *y*, *z*-axes are all at an equal angle [arccos(1/√3) rad] with respect to the Ir1-Ir2 bond and the *z*-axis lies in the Ir1-O1-Ir2 plane. The *x*, *y*, *z*-axes lie approximately along the Ir-O bonds in this setting. (c) RIXS map showing the intra-*t*<sub>2g</sub> and *t*<sub>2g</sub> → *e*<sub>g</sub> excitations.

Data were collected with a horizontal scattering geometry with the incident x-ray polarization parallel to the scattering plane ( $\pi$  channel). The sample was mounted such that [010] Ir chain direction and the [101] sample surface-normal are in the scattering plane. Data were collected using an incident x-ray angle  $\alpha$  close to 26° and a detector angle  $2\theta$  close to 90° unless otherwise specified.

We initially surveyed incident-energy-dependent RIXS at room temperature as shown in Fig. 1(c). The low energy excitations below 1.2 eV resonate at 11.215 keV and can be assigned to intra *t*<sub>2g</sub> transitions by comparison to previous work; *t*<sub>2g</sub> → *e*<sub>g</sub> transitions occur around 3.6 eV and resonant at higher incident energies [19, 30, 31]. A more detailed incident energy dependence was mapped at 40 K with 80 meV energy resolution [32], focusing on the low energy intra *t*<sub>2g</sub> excitations. The spectrum is plotted in Fig. 2(a,b), where 5 distinct peaks can be clearly identified. They are labeled A-E with energies 0.18 eV, 0.32 eV, 0.565 eV, 0.74 eV and 1.13 eV, respectively. These features show no appreciable dispersive behavior in their peak energies [see Fig. 2(c)] at various momentum transfer  $Q$  over almost one Brillouin zone in the chain direction, suggesting that the excitations are confined within a dimer and that coupling through the AlO<sub>4</sub>

tetrahedra can be neglected on these energy scales. We note that pure spin flip excitations are not observed here, almost certainly because they occur on a too low energy scale.

We use a two-site cluster model for Ir1 and Ir2 [see Fig. 1(b)] to simulate the measured RIXS spectrum. The *t*<sub>2g</sub> orbitals of Ir1 and Ir2 are defined with respect to the local Cartesian coordinates shown in Fig. 1(b). The ED-RIXS toolkit developed in the COMSCOPE project [33] is used to diagonalize the Hamiltonian and simulate the RIXS spectrum, with the real experimental geometry and polarization applied. The energy resolution is set to be 80 meV full width at half maximum (FWHM). More details of the RIXS simulation can be found in the Supplemental Materials [34].

To understand the electronic structure which gives rise to the observed excitations, we start with the non-physical condition where the Ir1-Ir2 hopping and the non-cubic crystal field (CF) are set to zero. With the octahedra decoupled, the electronic structure is determined by the spin-orbit coupling (SOC)  $\lambda$ , the on-site Coulomb  $U$  and the Hund's  $J_H$  interactions. We use a *t*<sub>2g</sub> Kanamori type Hamiltonian to treat  $U$  and  $J_H$ , which can be written as,

$$\hat{H}_U = U \sum_{\alpha} \hat{n}_{\alpha\uparrow} \hat{n}_{\alpha\downarrow} + U' \sum_{\alpha \neq \beta} \hat{n}_{\alpha\uparrow} \hat{n}_{\beta\downarrow} + U'' \sum_{\alpha < \beta, \sigma} \hat{n}_{\alpha\sigma} \hat{n}_{\beta\sigma} - J_H \sum_{\alpha \neq \beta} \hat{d}_{\alpha\uparrow}^{\dagger} \hat{d}_{\alpha\downarrow} \hat{d}_{\beta\downarrow}^{\dagger} \hat{d}_{\beta\uparrow} + J_H \sum_{\alpha \neq \beta} \hat{d}_{\alpha\uparrow}^{\dagger} \hat{d}_{\alpha\downarrow} \hat{d}_{\beta\downarrow} \hat{d}_{\beta\uparrow}^{\dagger}, \quad (1)$$

where,  $\alpha(\beta) = d_{zx}, d_{zy}, d_{xy}$  is the *t*<sub>2g</sub> orbital index.  $\sigma = \uparrow, \downarrow$  is the spin index.  $U' = U - 2J_H$  and  $U'' = U - 3J_H$ . With hopping forbidden, the electrons are localized to form  $|d^4\rangle$  on Ir1 and  $|d^5\rangle$  on Ir2, with atomic states  $|d^4, J_{\text{eff}} = 0, 1, 2, 2'\rangle$  and  $|d^5, J_{\text{eff}} = 1/2, 3/2\rangle$ , respectively. Excitations can happen within each atomic state sets, and their energies are determined by Hund's coupling and SOC. With  $J_H = 0.3$  eV and  $\lambda = 0.345$  eV, which are consistent with earlier work [35–38], the simulated RIXS spectrum is shown as the light blue curve in Fig. 3(c) where three peaks are found. The peak near B comes from the excitations from  $|d^4, J_{\text{eff}} = 0\rangle$  to  $|d^4, J_{\text{eff}} = 1\rangle$  states. The peak near C contains two excitations with very close energies, one is from  $|d^5, J_{\text{eff}} = 1/2\rangle$  to  $|d^5, J_{\text{eff}} = 3/2\rangle$  states and another is from  $|d^4, J_{\text{eff}} = 0\rangle$  to  $|d^4, J_{\text{eff}} = 2\rangle$  states. Peak E is determined by the excitations from  $|d^4, J_{\text{eff}} = 0\rangle$  to  $|d^4, J_{\text{eff}} = 2'\rangle$ . Obviously, our experimental observations have far richer features than this simulated RIXS spectrum at isolated atom level. The activation of the inter-site hopping will strongly mix the  $|d^4; d^5\rangle$  and  $|d^5; d^4\rangle$  configurations, which will not only tune the energy of the excitations but also create new de-localized states and excitation channels. Here, we use  $|d^{n_1}; d^{n_2}\rangle$  to represent a Direct Product State (DPS) of the dimer, where Ir1 has  $n_1$  electrons and Ir2 has  $n_2$  electrons.

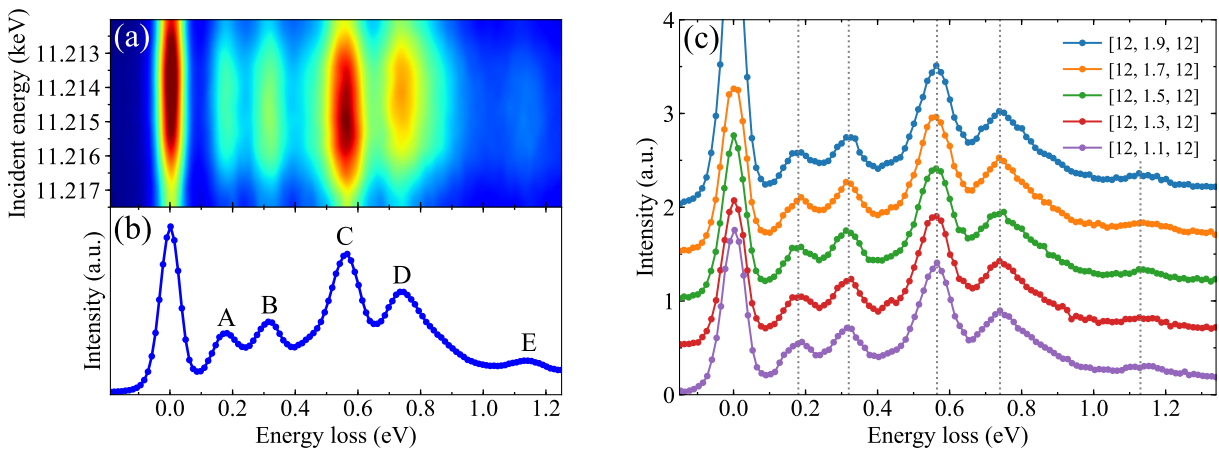


FIG. 2. (a) High-resolution RIXS map at 40 K. (b) The excitation spectrum integrated over  $\pm 2$  eV with respect to the resonant energy of 11215 eV. (c) Orbital excitations of  $\text{Ba}_5\text{AlIr}_2\text{O}_{11}$  show no significant  $\mathbf{Q}$ -dependence indicative of localized states.

To estimate the hopping and the non-cubic crystal field we performed a first-principles DFT calculation using Vienna Ab initio Simulation Package (VASP) [39–42] and fit a  $t_{2g}$  tight-binding (TB) Hamiltonian to the result using the maximally localized Wannier functions method [43, 44]. We set  $\lambda = U = J_H = 0$ , as they are included explicitly in our model later. For simplicity we assume a trigonal local CF for the  $\text{IrO}_6$  octahedra in  $\text{Ba}_5\text{AlIr}_2\text{O}_{11}$ . Under this approximation, the Hamiltonian  $\hat{V}^{12}$  for the hopping between Ir1 and Ir2 takes a simple form in the  $t_{2g}$  basis,

$$\hat{V}^{12} = \begin{matrix} & d_{z^2x_2} & d_{z^2y_2} & d_{x_2y_2} \\ \begin{matrix} d_{z_1x_1} \\ d_{z_1y_1} \\ d_{x_1y_1} \end{matrix} & \begin{pmatrix} -t & t' & -t \\ t' & -t & -t \\ -t & -t & t' \end{pmatrix} & + h.c. \end{matrix} \quad (2)$$

where,  $t$  and  $t'$  are the hopping parameters. Our DFT calculation gives  $t = 0.18$  eV, and  $t' \approx 0.2t$ . The on-site trigonal CF Hamiltonian is

$$\hat{H}_{\text{CF}}^{1(2)} = \begin{pmatrix} \mu_{1(2)} & -\delta & -\delta \\ -\delta & \mu_{1(2)} & -\delta \\ -\delta & -\delta & \mu_{1(2)} \end{pmatrix}, \quad (3)$$

where,  $\mu_1$  and  $\mu_2$  are the chemical potentials for Ir1 and Ir2, respectively. Their difference  $\Delta\mu = \mu_1 - \mu_2$  is about 0.1 eV. This chemical potential difference distinguishes the two inequivalent  $\text{IrO}_6$  octahedras [21, 45], and induces partial charge disproportionation in  $\text{Ba}_5\text{AlIr}_2\text{O}_{11}$ .  $\delta$  is estimated to be 0.03 eV from the DFT calculation. The two-site Ir1-Ir2 cluster Hamiltonian is diagonalized in the subspace with 9 electrons in total to get the energy spectrum.

For the isolated Ir1 and Ir2 condition discussed earlier, the energy levels (0-1.2 eV) of these DPS at  $\Delta\mu = 0$ ,  $\delta = 0$  and  $t = 0$  are shown as the red plateaus and labeled by S in Fig. 3(a). After turning on the hopping  $t$ , dimer

orbitals will form by superposition of the atomic orbitals of Ir1 and Ir2. As a result, the configurations  $|d^4; d^5\rangle$  and  $|d^5; d^4\rangle$  will mix with each other. With the DFT derived  $\{t, t', \Delta\mu, \delta\}$ , and the local interaction  $J_H = 0.3$  eV and  $\lambda = 0.345$  eV, the calculated energy levels of these delocalized dimer states are shown as blue lines in Fig. 3(a). As can be seen in Fig. 3(c), the calculated RIXS spectrum with these parameters agree quite well with our experimental observations. Peaks A and D, which were missing in the localized picture, now appear in the simulated RIXS spectrum as excitations between delocalized dimerized states. For example, peak A is from the excitation from the ground state to the first excited state. The weights of  $|d^4; d^5\rangle$  and  $|d^5; d^4\rangle$  configurations are respectively 0.608 and 0.392 in the ground state and 0.560 and 0.440 in the first excited state.

To further appreciate the competition between the atomic SOC  $\lambda$ , Hund's coupling  $J_H$  and the delocalization hopping  $t$ , the evolution of the energy spectrum of these dimer states as a function of hopping  $t$  is presented in Fig. 3(b). In this calculation, other parameters except hopping  $t$  are fixed. In Fig. 3(b), the solid lines are the relative energies of the dimer states, and underlying colormap represents the calculated corresponding RIXS intensities. We can see that each level S splits into many dimer states and the energy splitting increases as increasing  $t$ . In the small  $t$  regime, local on-site  $J_H$  and  $\lambda$  dominate the Hamiltonian, so the mixing mainly occurs within the same level S and the energy splitting is not far away from the center of each level S. When increasing  $t$ , it will compete with  $J_H$  and  $\lambda$  to induce more mixing between different levels S, which are reflected as the crossing of energy levels in Fig. 3(b). For example, the energy of the first excited state split from the level S0 increases at small  $t$  regime to a maximum and then decreases at  $t \gtrsim 0.12$ . Another state split from level S1 is pushed down to cross with it and has very similar energy.

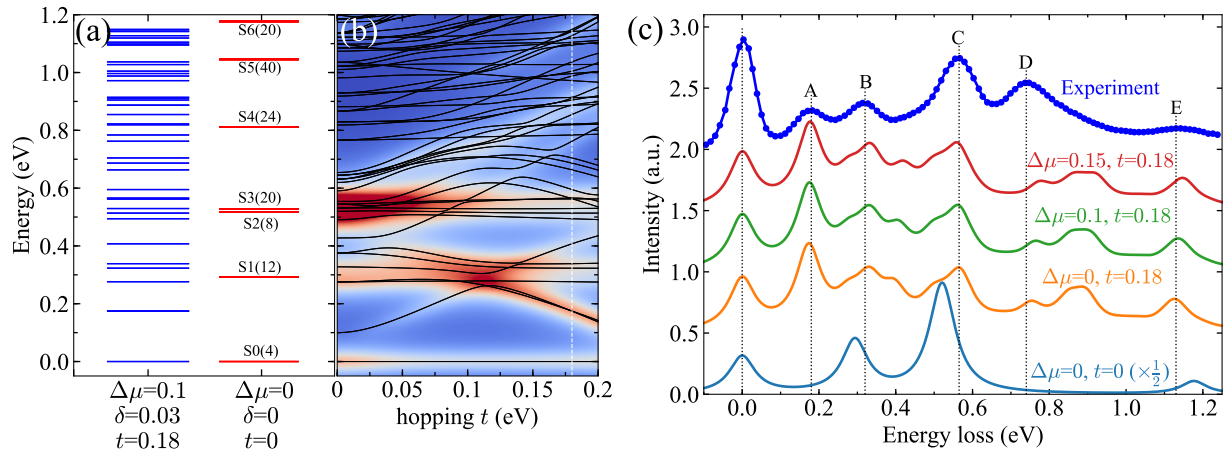


FIG. 3. (a) Illustration of the splitting of the trivial Direct Product State (DPS) after turning on hopping  $t$ . The letter S is used to label these DPS and the numbers in parentheses are their degeneracy. (b) The solid lines are the energy spectrum of the Ir-Ir cluster model as a function of hopping  $t$  at  $\Delta\mu = 0.1$  eV,  $\delta = 0.03$  eV, and the colormap indicates the corresponding simulated RIXS intensity. The vertical dotted line indicates  $t = 0.18$  eV. (c) The simulated RIXS spectrum at several chosen parameters and are compared with the experimental result,  $\delta = 0$  for the bottom light blue curve and  $\delta = 0.03$  for all others.

Besides peaks A-E, the calculated RIXS intensity also shows some shoulders around the main peaks which are not resolved in the experimental RIXS spectrum. They might be washed out by longer range hopping or itineracy not captured in the cluster model. We also find that the energy of the dimer states and the RIXS spectrum are not sensitive to  $\Delta\mu$  in the region  $\Delta\mu < t$  [see Fig. 3(c)], because  $t$  dominates the energy spectrum in this region and the energy splitting of the bonding and anti-bonding orbitals is as large as  $2.5t$ . At  $\Delta\mu = 0.1$  eV and  $t = 0.18$  eV, the calculated charge disproportionation between Ir1 and Ir2 is about 0.218 electrons, which is close to 0.3 electrons reported in previous DFT calculation [45].

Combining RIXS measurements and a DFT calculations, we show that the electronic structure of  $\text{Ba}_5\text{AlIr}_2\text{O}_{11}$  needs to be described by partially-delocalized dimer orbitals, rather than  $J_{\text{eff}} = 1/2$  atomic states in the strong SOC limit. It is interesting to notice that dimer orbitals can still occur in  $\text{Ba}_5\text{AlIr}_2\text{O}_{11}$  even if  $U$  is large, as due to the non-integer average Ir valence of 4.5, the Mott mechanism cannot stop hopping between the Ir sites. The dimerization process significantly changes the magnetic properties of  $\text{Ba}_5\text{AlIr}_2\text{O}_{11}$ . The calculated effective local moment per dimer is about  $1 \mu_B$  in  $\text{Ba}_5\text{AlIr}_2\text{O}_{11}$ , which is consistent with the experimental results [21], but is much smaller than the value  $1.732 \mu_B$  expected for two isolated Ir sites: a  $J_{\text{eff}} = 1/2$  on Ir2 and a  $J_{\text{eff}} = 0$  singlet on Ir1. It indicates that the symmetry of the magnetic order parameter has deviated from the ideal spherical symmetry. Indeed, unlike  $3d$  magnetic Mott insulators, where the order parameter can be described by pure local physics, it is common that the order parameter cannot be well described by a pure local

object in many iridates due to the extended orbitals and much stronger inter-site hoppings. For instance, reduced effective local moments have been observed in many  $d^5$  iridates, such as  $\text{Sr}_2\text{IrO}_4$  [46, 47],  $\text{Sr}_3\text{Ir}_2\text{O}_7$  [48] and pyrochlore iridates [49–51]. Another interesting case is the exotic magnetic moments found in some  $d^4$  iridates [52] where the local ground state is a non-magnetic singlet. This peculiar behavior is found to be caused by the virtual inter-site exchange process [53], so a local single atomic description is not appropriate here either. We also emphasize that the cluster model used in this work can be straightforwardly applied to simulate RIXS spectrum of the 6H-hexagonal oxides  $\text{Ba}_3\text{AB}_2\text{O}_9$  ( $A=\text{In, Y, Lu, Na}$  and  $B=\text{Ru, Ir}$ ) [13, 54, 55] and similar dimer excitations can be expected in these compounds. This theoretical method can also be generalized to study other systems with strong nonlocal electronic itineracy, such as the pyrochlore iridates, where possible low energy dimer excitations (around 0.1 eV) have been observed in RIXS spectrum [56–59].

In summary, we find new peaks corresponding to the excitations of dimer orbitals in the experimental RIXS spectrum of  $\text{Ba}_5\text{AlIr}_2\text{O}_{11}$ . The DFT calculations and the RIXS simulations confirm that the hopping strength between Ir1 and Ir2 in  $\text{Ba}_5\text{AlIr}_2\text{O}_{11}$  is indeed strong enough to form dimer orbitals and their excitations can be seen in the RIXS spectrum. We demonstrate that this combination of experimental and theoretical RIXS study can directly confirm the existence of delocalized dimer orbitals in  $\text{Ba}_5\text{AlIr}_2\text{O}_{11}$  and be used to explain the observed reduction of magnetic moment. This serves as an example and may open new directions to study delocalization in other dimerized strongly correlated materials by RIXS with widespread potential applications in molecules, ox-

ide heterostructures and even ultra-fast transient states.

We thank John Hill, Sergey Streltsov, Hu Miao and Keith Gilmore for discussions and support related to this project. Work at ShanghaiTech U. was partially supported by MOST of China under the grand No. 2016YFA0401000. R. W. was supported by international partnership program of Chinese Academy of Sciences under the grand No.112111KYSB20170059. This work received final support from the U.S. Department of Energy, Office of Basic Energy Sciences, Early Career Award Program under Award Number 1047478. Work at Brookhaven National Laboratory was supported by the U.S. Department of Energy, Office of Science, Office of Basic Energy Sciences, under Contract No. desc0012704. Work at Argonne is supported by the U.S. Department of Energy, Office of Science, under contract No. DE-AC-02-06CH11357. Y.W. and G.K. was supported by the US Department of energy, Office of Science, Basic Energy Sciences as a part of the Computational Materials Science Program through the Center for Computational Design of Functional Strongly Correlated Materials and Theoretical Spectroscopy. G.C. acknowledges the NSF support via NSF grant DMR-1712101.

---

\* yilinwang@bnl.gov

† mdean@bnl.gov

‡ liuxr@shanghaitech.edu.cn

- [1] B. Keimer and J. E. Moore, “The physics of quantum materials,” *Nature Physics* **13**, 1045 (2017).
- [2] Daniel I. Khomskii, *Transition Metal Compounds* (Cambridge University Press, 2014).
- [3] Jiří Chaloupka, George Jackeli, and Giniyat Khaliullin, “Kitaev-Heisenberg Model on a Honeycomb Lattice: Possible Exotic Phases in Iridium Oxides  $A_2IrO_3$ ,” *Phys. Rev. Lett.* **105**, 027204 (2010).
- [4] Yoshihiko Okamoto, Minoru Nohara, Hiroko Aruga-Katori, and Hidenori Takagi, “Spin-Liquid State in the  $S = 1/2$  Hyperkagome Antiferromagnet  $Na_4Ir_3O_8$ ,” *Phys. Rev. Lett.* **99**, 137207 (2007).
- [5] Leon Balents, “Spin liquids in frustrated magnets,” *Nature* **464**, 199 (2010).
- [6] Michael J. Lawler, Arun Paramakanti, Yong Baek Kim, and Leon Balents, “Gapless Spin Liquids on the Three-Dimensional Hyperkagome Lattice of  $Na_4Ir_3O_8$ ,” *Phys. Rev. Lett.* **101**, 197202 (2008).
- [7] Yi Zhou, Patrick A. Lee, Tai-Kai Ng, and Fu-Chun Zhang, “ $Na_4Ir_3O_8$  as a 3D Spin Liquid with Fermionic Spinons,” *Phys. Rev. Lett.* **101**, 197201 (2008).
- [8] Dmytro Pesin and Leon Balents, “Mott physics and band topology in materials with strong spin-orbit interaction,” *Nature Physics* **6**, 376 (2010).
- [9] Atsuo Shitade, Hosho Katsura, Jan Kuneš, Xiao-Liang Qi, Shou-Cheng Zhang, and Naoto Nagaosa, “Quantum spin Hall effect in a transition metal oxide  $Na_2IrO_3$ ,” *Physical review letters* **102**, 256403 (2009).
- [10] Fa Wang and T. Senthil, “Twisted Hubbard Model for  $Sr_2IrO_4$ : Magnetism and Possible High Temperature Superconductivity,” *Phys. Rev. Lett.* **106**, 136402 (2011).
- [11] Gang Cao and Pedro Schlottmann, “The challenge of spin-orbit-tuned ground states in iridates: a key issues review,” *Reports on Progress in Physics* **81**, 042502 (2018).
- [12] S. K. Panda, S. Bhowal, Ying Li, S. Ganguly, Roser Valentí, L. Nordström, and I. Dasgupta, “Electronic structure and spin-orbit driven magnetism in  $d^{4.5}$  insulator  $Ba_3Yr_2O_9$ ,” *Phys. Rev. B* **92**, 180403 (2015).
- [13] Tusharkanti Dey, M. Majumder, J. C. Orain, A. Senyshyn, M. Prinz-Zwick, S. Bachus, Y. Tokiwa, F. Bert, P. Khuntia, N. Büttgen, A. A. Tsirlin, and P. Gegenwart, “Persistent low-temperature spin dynamics in the mixed-valence iridate  $Ba_3InIr_2O_9$ ,” *Phys. Rev. B* **96**, 174411 (2017).
- [14] Jason S. Gardner, Michel J. P. Gingras, and John E. Greedan, “Magnetic pyrochlore oxides,” *Rev. Mod. Phys.* **82**, 53–107 (2010).
- [15] Sergey V. Streltsov and Daniel I. Khomskii, “Covalent bonds against magnetism in transition metal compounds,” *Proceedings of the National Academy of Sciences* **113**, 10491–10496 (2016).
- [16] M. Ye, H.-S. Kim, J.-W. Kim, C.-J. Won, K. Haule, D. Vanderbilt, S.-W. Cheong, and G. Blumberg, “Covalency-driven collapse of strong spin-orbit coupling in face-sharing iridium octahedra,” *ArXiv e-prints* (2018), arXiv:1808.10407 [cond-mat.str-el].
- [17] I. I. Mazin, Harald O. Jeschke, Kateryna Foyevtsova, Roser Valentí, and D. I. Khomskii, “ $Na_2IrO_3$  as a Molecular Orbital Crystal,” *Phys. Rev. Lett.* **109**, 197201 (2012).
- [18] Jun-ichi Igarashi and Tatsuya Nagao, “Analysis of resonant inelastic x-ray scattering from  $Sr_2IrO_4$  in an itinerant-electron approach,” *Phys. Rev. B* **90**, 064402 (2014).
- [19] X Liu, Vamshi M Katukuri, L Hozoi, Wei-Guo Yin, MPM Dean, MH Upton, Jungho Kim, D Casa, A Said, T Gog, *et al.*, “Testing the validity of the strong spin-orbit-coupling limit for octahedrally coordinated iridate compounds in a model system  $Sr_3CuIrO_6$ ,” *Physical review letters* **109**, 157401 (2012).
- [20] H. Gretarsson, J. P. Clancy, X. Liu, J. P. Hill, Emil Bozin, Yogesh Singh, S. Manni, P. Gegenwart, Jungho Kim, A. H. Said, D. Casa, T. Gog, M. H. Upton, Heung-Sik Kim, J. Yu, Vamshi M. Katukuri, L. Hozoi, Jeroen van den Brink, and Young-June Kim, “Crystal-Field Splitting and Correlation Effect on the Electronic Structure of  $A_2IrO_3$ ,” *Phys. Rev. Lett.* **110**, 076402 (2013).
- [21] Jsaminka Terzic, JC Wang, Feng Ye, WH Song, SJ Yuan, Saicharan Aswartham, Lance E DeLong, SV Streltsov, Daniel I Khomskii, and Gang Cao, “Coexisting charge and magnetic orders in the dimer-chain iridate  $Ba_5AlIr_2O_{11}$ ,” *Physical Review B* **91**, 235147 (2015).
- [22] L J P Ament, M van Veenendaal, T P Devereaux, J P Hill, and J van den Brink, “Resonant inelastic x-ray scattering studies of elementary excitations,” *Rev. Mod. Phys.* **83**, 705 (2011).
- [23] A. Föhlisch, M. Nyberg, J. Hasselström, O. Karis, L. G. M. Pettersson, and A. Nilsson, “How Carbon Monoxide Adsorbs in Different Sites,” *Phys. Rev. Lett.* **85**, 3309–3312 (2000).
- [24] M. P. M. Dean, R S Springell, C Monney, K J Zhou, J Pereiro, I Božović, Bastien Dalla Piazza, H M Rønnow, E Morenzoni, J van den Brink, *et al.*, “Spin excitations in

- a single  $\text{La}_2\text{CuO}_4$  layer,” *Nat. Mater.* **11**, 850–854 (2012).
- [25] A. Lupascu, J. P. Clancy, H. Gretarsson, Zixin Nie, J. Nichols, J. Terzic, G. Cao, S. S. A. Seo, Z. Islam, M. H. Upton, Jungho Kim, D. Casa, T. Gog, A. H. Said, Vamshi M. Katukuri, H. Stoll, L. Hozoi, J. van den Brink, and Young-June Kim, “Tuning Magnetic Coupling in  $\text{Sr}_2\text{IrO}_4$  Thin Films with Epitaxial Strain,” *Phys. Rev. Lett.* **112**, 147201 (2014).
- [26] M. P. M. Dean, Y. Cao, X. Liu, S. Wall, D. Zhu, R. Mankowsky, V. Thampy, X. M. Chen, J. G. Vale, D. Casa, Jungho Kim, A. H. Said, P. Juhas, R. Alonso-Mori, J. M. Glowia, A. Robert, J. Robinson, M. Sikorski, S. Song, M. Kozina, H. Lemke, L. Patthey, S. Owada, T. Katayama, M. Yabashi, Yoshikazu Tanaka, T. Togashi, J. Liu, C. Rayan Serrao, B. J. Kim, L. Huber, C. L. Chang, D. F. McMorrow, M. Först, and J. P. Hill, “Ultrafast energy- and momentum-resolved dynamics of magnetic correlations in the photo-doped Mott insulator  $\text{Sr}_2\text{IrO}_4$ ,” *Nature Materials* **15**, 601 (2016).
- [27] D Meyers, Yue Cao, G Fabbris, Neil J Robinson, Lin Hao, C Frederick, N Traynor, J Yang, Jiaqi Lin, MH Upton, *et al.*, “Magnetism in artificial Ruddlesden-Popper iridates leveraged by structural distortions,” arXiv preprint arXiv:1707.08910 (2017).
- [28] Cao Gang and Lance De-Long, *Frontiers of 4d-and 5d-transition Metal Oxides* (World Scientific, 2013).
- [29] Yu V Shvyd’ko, JP Hill, CA Burns, DS Coburn, B Brajuskovic, D Casa, K Goetze, T Gog, R Khachatryan, J-H Kim, *et al.*, “MERIX: Next generation medium energy resolution inelastic X-ray scattering instrument at the APS,” *Journal of Electron Spectroscopy and Related Phenomena* **188**, 140–149 (2013).
- [30] K. Ishii, I. Jarrige, M. Yoshida, K. Ikeuchi, J. Mizuki, K. Ohashi, T. Takayama, J. Matsuno, and H. Takagi, “Momentum-resolved electronic excitations in the Mott insulator  $\text{Sr}_2\text{IrO}_4$  studied by resonant inelastic x-ray scattering,” *Phys. Rev. B* **83**, 115121 (2011).
- [31] M. Moretti Sala, K. Ohgushi, A. Al-Zein, Y. Hirata, G. Monaco, and M. Krisch, “ $\text{CaIrO}_3$ : A Spin-Orbit Mott Insulator Beyond the  $j_{\text{eff}} = 1/2$  Ground State,” *Phys. Rev. Lett.* **112**, 176402 (2014).
- [32] Higher resolution data was taken with 30 meV energy resolution, but the this does not reveal any new features.
- [33] “COMSCOPE project,” <https://www.bnl.gov/comscope/index.php>.
- [34] See Supplemental Material at [url] for details of the DFT calculations and RIXS cross-section. The Supplemental Material includes Refs. [22, 40? ? –42].
- [35] I. I. Mazin, S. Manni, K. Foyevtsova, Harald O. Jeschke, P. Gegenwart, and Roser Valentí, “Origin of the insulating state in honeycomb iridates and rhodates,” *Phys. Rev. B* **88**, 035115 (2013).
- [36] Bo Yuan, JP Clancy, AM Cook, CM Thompson, J Greedan, G Cao, BC Jeon, TW Noh, MH Upton, D Casa, *et al.*, “Determination of Hund’s coupling in 5 d oxides using resonant inelastic x-ray scattering,” *Physical Review B* **95**, 235114 (2017).
- [37] B. J. Kim and Giniyat Khaliullin, “Resonant inelastic x-ray scattering operators for  $t_{2g}$  orbital systems,” *Phys. Rev. B* **96**, 085108 (2017).
- [38] Arun Paramakanti, David J. Singh, Bo Yuan, Diego Casa, Ayman Said, Young-June Kim, and A. D. Christianson, “Spin-orbit coupled systems in the atomic limit: rhenates, osmates, iridates,” *Phys. Rev. B* **97**, 235119 (2018).
- [39] G. Kresse and J. Furthmüller, “Efficient iterative schemes for *ab initio* total-energy calculations using a plane-wave basis set,” *Phys. Rev. B* **54**, 11169–11186 (1996).
- [40] P. E. Blöchl, “Projector augmented-wave method,” *Phys. Rev. B* **50**, 17953–17979 (1994).
- [41] G. Kresse and D. Joubert, “From ultrasoft pseudopotentials to the projector augmented-wave method,” *Phys. Rev. B* **59**, 1758–1775 (1999).
- [42] John P. Perdew, Kieron Burke, and Matthias Ernzerhof, “Generalized Gradient Approximation Made Simple,” *Phys. Rev. Lett.* **77**, 3865–3868 (1996).
- [43] Nicola Marzari, Arash A. Mostofi, Jonathan R. Yates, Ivo Souza, and David Vanderbilt, “Maximally localized Wannier functions: Theory and applications,” *Rev. Mod. Phys.* **84**, 1419–1475 (2012).
- [44] Arash A. Mostofi, Jonathan R. Yates, Young-Su Lee, Ivo Souza, David Vanderbilt, and Nicola Marzari, “Wannier90: A tool for obtaining maximally-localised Wannier functions,” *Computer Physics Communications* **178**, 685 – 699 (2008).
- [45] Sergey V. Streltsov, Gang Cao, and Daniel I. Khomskii, “Suppression of magnetism in  $\text{Ba}_5\text{AlIr}_2\text{O}_{11}$ : Interplay of Hund’s coupling, molecular orbitals, and spin-orbit interaction,” *Phys. Rev. B* **96**, 014434 (2017).
- [46] G. Cao, J. Bolivar, S. McCall, J. E. Crow, and R. P. Guertin, “Weak ferromagnetism, metal-to-nonmetal transition, and negative differential resistivity in single-crystal  $\text{Sr}_2\text{IrO}_4$ ,” *Phys. Rev. B* **57**, R11039–R11042 (1998).
- [47] B. J. Kim, Hosub Jin, S. J. Moon, J.-Y. Kim, B.-G. Park, C. S. Leem, Jaejun Yu, T. W. Noh, C. Kim, S.-J. Oh, J.-H. Park, V. Durairaj, G. Cao, and E. Rotenberg, “Novel  $J_{\text{eff}} = 1/2$  Mott State Induced by Relativistic Spin-Orbit Coupling in  $\text{Sr}_2\text{IrO}_4$ ,” *Phys. Rev. Lett.* **101**, 076402 (2008).
- [48] G. Cao, Y. Xin, C. S. Alexander, J. E. Crow, P. Schlottmann, M. K. Crawford, R. L. Harlow, and W. Marshall, “Anomalous magnetic and transport behavior in the magnetic insulator  $\text{Sr}_3\text{Ir}_2\text{O}_7$ ,” *Phys. Rev. B* **66**, 214412 (2002).
- [49] Jun J. Ishikawa, Eoin C. T. O’Farrell, and Satoru Nakatsuji, “Continuous transition between antiferromagnetic insulator and paramagnetic metal in the pyrochlore iridate  $\text{Eu}_2\text{Ir}_2\text{O}_7$ ,” *Phys. Rev. B* **85**, 245109 (2012).
- [50] M. C. Shapiro, Scott C. Riggs, M. B. Stone, C. R. de la Cruz, S. Chi, A. A. Podlesnyak, and I. R. Fisher, “Structure and magnetic properties of the pyrochlore iridate  $\text{Y}_2\text{Ir}_2\text{O}_7$ ,” *Phys. Rev. B* **85**, 214434 (2012).
- [51] S. M. Disseler, Chetan Dhital, T. C. Hogan, A. Amato, S. R. Giblin, Clarina de la Cruz, A. Daoud-Aladine, Stephen D. Wilson, and M. J. Graf, “Magnetic order and the electronic ground state in the pyrochlore iridate  $\text{Nd}_2\text{Ir}_2\text{O}_7$ ,” *Phys. Rev. B* **85**, 174441 (2012).
- [52] G. Cao, T. F. Qi, L. Li, J. Terzic, S. J. Yuan, L. E. DeLong, G. Murthy, and R. K. Kaul, “Novel Magnetism of  $\text{Ir}^{5+}(5d^4)$  Ions in the Double Perovskite  $\text{Sr}_2\text{YIrO}_6$ ,” *Phys. Rev. Lett.* **112**, 056402 (2014).
- [53] Giniyat Khaliullin, “Excitonic Magnetism in Van Vleck-type  $d^4$  Mott Insulators,” *Phys. Rev. Lett.* **111**, 197201 (2013).
- [54] D. Ziat, A. A. Aczel, R. Sinclair, Q. Chen, H. D. Zhou, T. J. Williams, M. B. Stone, A. Verrier, and J. A. Quilliam, “Frustrated spin- $\frac{1}{2}$  molecular magnetism in the

- mixed-valence antiferromagnets  $Ba_3MRu_2O_9$  ( $M = \text{In}, \text{Y}, \text{Lu}$ ),” *Phys. Rev. B* **95**, 184424 (2017).
- [55] Simon A. J. Kimber, Mark S. Senn, Simone Fratini, Hua Wu, Adrian H. Hill, Pascal Manuel, J. Paul Attfield, Dimitri N. Argyriou, and Paul F. Henry, “Charge Order at the Frontier between the Molecular and Solid States in  $Ba_3NaRu_2O_9$ ,” *Phys. Rev. Lett.* **108**, 217205 (2012).
- [56] J. P. Clancy, H. Gretarsson, E. K. H. Lee, Di Tian, J. Kim, M. H. Upton, D. Casa, T. Gog, Z. Islam, Byung-Gu Jeon, Kee Hoon Kim, S. Desgreniers, Yong Baek Kim, S. J. Julian, and Young-June Kim, “X-ray scattering study of pyrochlore iridates: Crystal structure, electronic, and magnetic excitations,” *Phys. Rev. B* **94**, 024408 (2016).
- [57] C. Donnerer, M. C. Rahn, M. Moretti Sala, J. G. Vale, D. Pincini, J. Strempler, M. Krisch, D. Prabhakaran, A. T. Boothroyd, and D. F. McMorrow, “All-in-all-Out Magnetic Order and Propagating Spin Waves in  $Sm_2Ir_2O_7$ ,” *Phys. Rev. Lett.* **117**, 037201 (2016).
- [58] Sae Hwan Chun, Bo Yuan, Diego Casa, Jungho Kim, Chang-Yong Kim, Zhaoming Tian, Yang Qiu, Satoru Nakatsuji, and Young-June Kim, “Magnetic Excitations across the Metal-Insulator Transition in the Pyrochlore Iridate  $Eu_2Ir_2O_7$ ,” *Phys. Rev. Lett.* **120**, 177203 (2018).
- [59] S. Calder, J. G. Vale, N. A. Bogdanov, X. Liu, C. Donnerer, M. H. Upton, D. Casa, A. H. Said, M. D. Lumsden, Z. Zhao, J.-Q. Yan, D. Mandrus, S. Nishimoto, J. van den Brink, J. P. Hill, D. F. McMorrow, and A. D. Christianson, “Spin-orbit-driven magnetic structure and excitation in the 5d pyrochlore  $Cd_2Os_2O_7$ ,” *Nature Communications* **7**, 11651 (2016).